ICAS-94-3.8.2

WIND TUNNEL BLOCKAGE EFFECTS ON THE AGARD B MODEL IN TRANSONIC FLOW

Giovanni Lombardi
Department of Aerospace Engineering, University of Pisa, Italy

Mauro Morelli
Medium Speed Wind Tunnel, CSIR, South Africa

Summary

The effects of the walls of a test section on a model in transonic flow were investigated, by using the AGARD Calibration Model B. Tests were carried out in a closed circuit pressurised tunnel, with a confined square test section of 1.5 m width, with tapered slots giving a 5% porosity. Two models with different dimensions were used, with 0.78 percent and 0.05 percent blockage ratios. Longitudinal aerodynamic characteristics were analysed, by means of measurements performed at varying angles of attack (up to 24 degrees) and Mach numbers from 0.3 to 1.2. In some flow conditions wall interference effects were probably present. However, the forces dependent on the pressure distribution were likely to be related to the same factors, and therefore the above effects tended to disappear when longitudinal stability and lift dependent drag were analysed as a function of lift characteristics. Anyhow, the drag rise Mach number evaluation seems be fully free from blockage effects. Summing up, the dimensions of the tested larger model can be considered to be the largest reasonable ones for industrial applications, but, probably, not sufficiently small when high accuracy is required.

Nomenclature

b	model span (m)
c_b	chord at the body-wing junction (m)
c_{ma}	mean aerodynamic chord (m)
c_r	Root chord (m)
C_D	forebody drag coefficient
C_{Dmin}	minimum value for C_D for a given Mach number
C_{D0}	zero lift drag coefficient for a given Mach number
C_L	forebody lift coefficient
C_M	forebody pitching moment coefficient
d	diameter of the support sting (m)
D	model fuselage diameter (m)
K	coefficient in the law $C_D = C_{Dmin} + K\,C_L^2$
L_a	base to wing trailing edge distance (m)
L_f	ogive length (m)
L_t	total length (m)
M	Mach number
P	confidence level
S_w	gross wing area (m^2)
w	test section width (m)
x_{ref}	distance of the moment reference point from the model base (m)
α	angle of attack (degree)

Introduction

The interference on the flow field around a model caused by wind tunnel walls is known to be one of the main sources of error affecting the accuracy of experimental data. The classical correction criteria are not satisfactory for a really accurate data correction, being based on insufficiently representative theoretical linear models (see, e.g., [1]), whose validity is limited to low velocities and angles of attack; however, even in these conditions, the accuracy of these criteria is not high, since they do not account of physical tunnel characteristics (i.e. fillets, re-entry doors, etc., [2]). With the introduction of the ventilated test section for high-speed subsonic and transonic testing, new procedures have been devised to extend the classical wall interference methods for correcting model test data. Because of the complex nature of the interference, a satisfactory general analytical solution to this problem for ventilated walls is far from being achieved. More recently, new correction methods were introduced, based on more complex procedures, coupling measurements - typically pressure and/or velocity on the wall or in the field - with numerical calculations (see, e.g., [3], [4]). Anyway, these procedures experience difficulties because of the small quantities to be measured, the uncertainty of the devices used to make the measurements and the interference from other sources, [2], as well as because of the complexity of flow calculation. Furthermore, in three-dimensional problems, the number of field measurements necessary for a proper wall correction evaluation is so large that it yields an experimental procedure practically very difficult to perform - at least as regard industrial applications. This holds particularly for transonic conditions or for high angles of attack, because linear models are not valid, and it is almost impossible to use a reliable numerical code.

The above considerations explain why limiting model dimensions, as much as possible, remains the best way to avoid unacceptable errors. On the other hand, the importance of testing the largest possible model is evident, not only to maximise the Reynolds number but, especially, to improve the accuracy of force measurement and of the model itself, as clearly shown in [5]. Thus, it is important to have reliable criteria for choosing model size, [6]; advancing knowledge on this matter is the main purpose of the present research activity.

The effects of the walls of the wind tunnel on a model in transonic flow were investigated, by using the AGARD Calibration Model B, specified in [7] and schematically showed in fig. 1.

It is an ogive-cylinder body with a delta wing having a symmetrical circular arc airfoil section, already tested in many different wind tunnels (see, e.g., [8]). Two models, with different dimensions, were used. The first one (named "large" model) had a nominal diameter (fig. 1) D=150 mm, with a corresponding blockage, at zero angle of attack, of 0.78 percent and a model to test section width ratio, b/w, of 0.400; the other one (named "small" model) had a nominal diameter D=38.5 mm, with a corresponding blockage of 0.05 percent and a b/w ratio of 0.103. Because of the very low blockage of the small model, the latter could be considered actually free of wall interference. The dimensions of the large model were chosen as indicatively the largest possible for the test section geometry, [9].

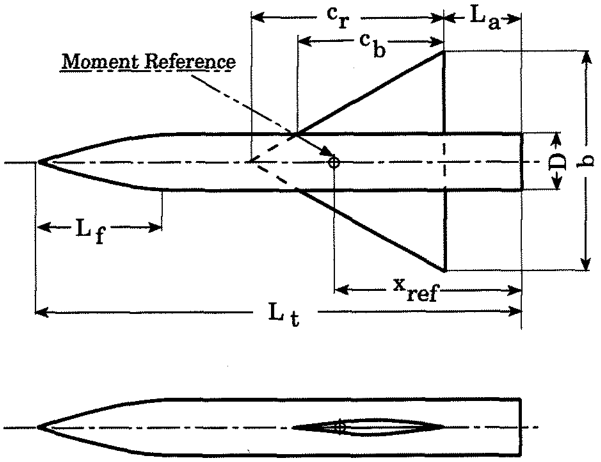

Nominal dimensions

L_t	= 8.5 D	x_{ref}	= 3.148 D
L_f	= 3 D	c_b	= 2.598 D
L_a	= 1.402 D	b	= 4 D

fig. 1 - The AGARD B model

To avoid differences caused by different flow characteristics, which may significantly affect forces (particularly, the turbulence scale and intensity, see, e.g., [10]), the test conditions were kept the same for both models; in this way, the two models were tested at different Reynolds numbers, but this influence can be considered to be (at least qualitatively) known - particularly for the tested model, which had been extensively studied in many different conditions.

Experimental Set-Up

Tests were carried out in the Medium Speed Wind Tunnel of the CSIR Laboratories, in South Africa. This is a closed circuit variable density transonic wind-tunnel. Its operational speed ranges from M=0.25 to M=1.5 with pressure varying from 20 kPa to 250 kPa; Reynolds number can be changed by modifying the pressure. The test section has a 1.5m x 1.5m square cross section, 4.5m in length. All four walls are equally longitudinally slotted for a total porosity of 5%, following the scheme in fig. 2; the lateral walls are parallel, while the upper and lower ones are slightly diverging, 0.7 degrees each one, starting from the test section inlet.

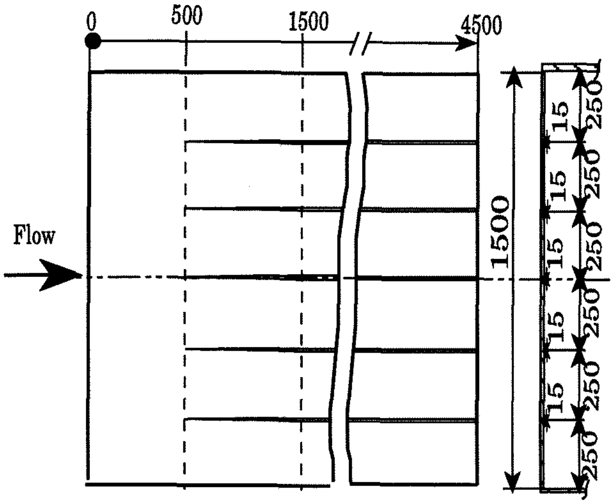

All dimensions in millimeters

Note: the slots on the four walls are positioned in the same way

fig. 2 - Definition of the walls of the test section

The main flow characteristics in the test section are summarised in tab. 1, derived from the complete calibration of the wind tunnel, as presented in [11].

Stability of Mach number with time	σ_{Mt} δ 0.0014	
Stability of stagnation pressure with time	σ_{P_0} δ 0.0012	KPa
Stability of stagnation temperature with time	σ_{T_0} δ 2	K
Humidity leveldewpoint below tunnel static temperature	2	K
Spatial variation of Mach number (subsonic)	σ_Mδ 0.002	
(supersonic)	σ_Mδ 0.004	
Spatial variation of flow angularity (subsonic)	σ_μδ 0.15	
(supersonic)	σ_μδ 0.30	
Acoustic pressure coefficient fluctuation	Δc_p δ 0.01	
Acoustic fluctuation frequency content	$[n\ F(n)]^{1/2}$ δ 0.007	
Turbulence level (low Mach)	σ_u/U δ 0.001	
(high Mach)	σ_u/U δ 0.002	

Tab.1- Main flow characteristics in the test section

The models were assembled on the main model support (fig. 3), which consists of a pitch sector with a roll head that transmits the attitude movements to the model. They were connected through internal balances onto a sting, and base pressure probes were fitted onto both models.

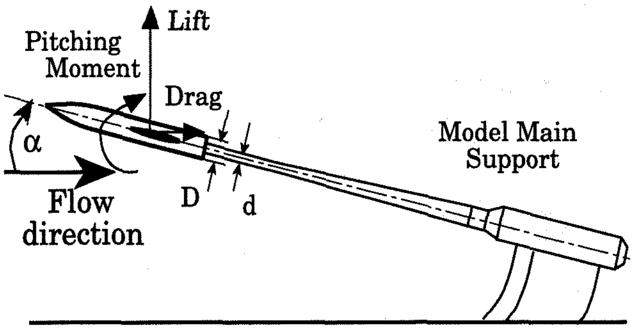

Fig. 3 - Scheme of the montage and reference system

On the large model, two pressure orifices were fitted in diametrically opposite positions on the sting, at the base of the model, while on the small model a single orifice was used to measure the base pressure. The mounting scheme is identical for the two models; in particular the sting diameter to base diameter ratio (d/D) for the large model is 0.500, and for the small model 0.506. Two internal, six component strain gauge balances were used to measure the forces on the models.

Both models were tested under the same environmental conditions and attitudes, namely, from M=0.3 to M=0.9 in 0.1 steps, from M=0.95 to M=1.1 in 0.05 steps and at M=1.2. Under these conditions the Reynolds number, referred to the model total length L_t, varied from $9.2\text{x}10^6$ to $1.7\text{x}10^7$ for the large model, and from $2.4\text{x}10^6$ to $4.5\text{x}10^6$ for the small model.

The models were tested at pitch angles that ranged from -4 to 24 for Mach numbers up to 0.7, and from -4 to 17.5 for the remaining Mach numbers. In these conditions neither model oscillation was detected during the angle of attack sweep. The measured body axis forces were converted into drag and lift values, and the effects of the base pressure were eliminated, i.e., only the forces acting on the forebody were considered.

The balance data were acquired through a NEFF system 620 series 500 provided with a 16-bit A/D converter. The pressure data were acquired through a Scanivalve 20 C system with a 12-bit A/D converter.

The adopted reference system is shown in fig. 3. The force coefficients were non-dimensionalised with the dynamic pressure and the gross wing

			LARGE MODEL		SMALL MODEL	
			Nominal	Real	Nominal	Real
Diameter	D	mm	150	150	38.5	38.5
Total length	L_t	mm	1275	1289.88	327.5	328.44
Wing span	b	mm	600	598.68	154	152.45
Chord at the body-wing junction	c_b	mm	389.7	389.30	100.03	100.00
Base to wing trailing edge distance	L_a	mm	210.3	210.20	53.98	54.05
Root chord	c_r	mm		519.60		133.36
Mean aerodynamic chord	c_{ma}	mm		346.4		89.0
c_{ma} quarter point (from base)	x_{ref}	mm		472.2		121.2
Gross wing area	S_w	mm^2		155537.1		10165.7
Wetted wing area		mm^2		89354.6		5185.0
Model volume		m^3		.0172		.000291
Blockage factor at $\alpha=0$				0.78 %		0.05 %
Blockage factor at $\alpha=24$				4.66 %		0.30 %
Wing span to tunnel width ratio	b/w			.400		.103
Sting to model diameter ratio	d/D			.500		.506

symbols are referred to fig. 1

Tab. 2 - Nominal and real dimensions of the two models

area (S_w), the moment coefficients with the dynamic pressure, the gross wing area and the mean aerodynamic chord (c_{ma}), and were referred to the quarter chord point of the mean aerodynamic chord.

The quality control inspection carried out on the models is fully described in [12]; it was accomplished on a model 2202 DEA IOTA Coordinate Measuring Machine with computerised measuring and recording capability. In tab. 2 the nominal and real dimensions of the two models are reported, the uncertainty in the linear measurements being less than 0.01 mm.

An automatic Mach controller maintained a constant Mach number, compensating for Mach number variations such as those induced by the model pitch cycle.

C_L	0.1			0.6			1.1		
M	balance bias	total bias	precision	balance bias	total bias	precision	balance bias	total bias	precision
0.3	.0041	.0073	.0019	.0041	.0068	.0016	.0041	.0063	.0015
1.0	.0013	.0038	.0015	.0013	.0031	.0012	.0013	.0028	.0011
1.2	.0011	.0028	.0013	.0011	.0025	.0010	.0011	.0023	.0009

C_M	0.02			0.07			.12		
M	balance bias	total bias	precision	balance bias	total bias	precision	balance bias	total bias	precision
0.3	.00072	.00188	.00042	.00072	.00178	.00038	.00072	.00172	.00033
1.0	.00020	.00061	.00036	.00020	.00057	.00032	.00020	.00053	.00028
1.2	.00017	.00054	.00031	.00017	.00046	.00024	.00017	.00041	.00021

C_D	0.1			0.2			0.3		
M	balance bias	total bias	precision	balance bias	total bias	precision	balance bias	total bias	precision
0.3	.0046	.0078	.0021	.0046	.0074	.0016	.0046	.0069	.0014
1.0	.0017	.0042	.0016	.0017	.0036	.0015	.0017	.0032	.0012
1.2	.0013	.0031	.0015	.0013	.0028	.0012	.0013	.0025	.0012

Tab. 3 - Bias and precision uncertainty level in the force coefficients evaluation procedure (P=0.95)
LARGE MODEL

C_L	0.1			0.6			1.1		
M	balance bias	total bias	precision	balance bias	total bias	precision	balance bias	total bias	precision
0.3	.0032	.0082	.0023	.0032	.0073	.0019	.0032	.0071	.0017
1.0	.0010	.0047	.0016	.0010	.0037	.0015	.0010	.0033	.0014
1.2	.0009	.0033	.0013	.0009	.0031	.0012	.0009	.0030	.0013

C_M	0.02			0.07			.12		
M	balance bias	total bias	precision	balance bias	total bias	precision	balance bias	total bias	precision
0.3	.00064	.00198	.00045	.00064	.00183	.00051	.00064	.00185	.00036
1.0	.00018	.00072	.00038	.00018	.00061	.00039	.00018	.00058	.00031
1.2	.00015	.00067	.00035	.00015	.00056	.00028	.00015	.00049	.00028

C_D	0.1			0.2			0.3		
M	balance bias	total bias	precision	balance bias	total bias	precision	balance bias	total bias	precision
0.3	.0041	.0083	.0024	.0041	.0078	.0019	.0041	.0074	.0018
1.0	.0014	.0045	.0019	.0014	.0039	.0018	.0014	.0037	.0017
1.2	.0011	.0033	.0017	.0011	.0033	.0016	.0011	.0029	.0017

Tab. 4 - Bias and precision uncertainty level in the force coefficients evaluation procedure (P=0.95)
SMALL MODEL

The uncertainty in Mach number was 0.002, [13]; that in the angle of attack positioning was less than 0.1 degrees, and data were corrected for sting deflections. The total uncertainties in the data that can be attributed to instrumentation errors (forces, dynamic pressure and base pressure measurements), reference dimension evaluation (surfaces, lengths and moment reduction points) and data acquisition procedure are shown, for each force component, in tab. 3 (large model), tab. 4 (small model) and tab. 5 (zero lift drag), expressed as coefficient uncertainty; the uncertainties were determined as suggested in [14], for a confidence level of 95 percent.

	LARGE model		
M	balance bias	total bias	precision
0.3	.0031	.0046	.0019
1.0	.0011	.0029	.0013
1.2	.0009	.0024	.0011
	SMALL model		
0.3	.0033	.0045	.0025
1.0	.0014	.0029	.0018
1.2	.0011	.0025	.0015

Tab. 5 - Bias and precision uncertainty level in the C_{D0} measurement procedure (P=0.95)

It has to be noted that, because of the use of the wind tunnel under identical flow conditions (for a given Mach number), the bias uncertainty should not be considered in its entirety when comparing the two model, as including a fraction (that dependent on flow measurements and on the evaluation of the model dimensions) that was the same in both cases. For this reason in the tables the bias error is reported both as total values and as balance bias; however, only the latter gives the uncertainty in the comparisons.

Analysis of the results

Preliminary tests performed at different Reynolds numbers showed that not significant effects of this parameter, especially on the pressure dependent forces, were present; this was probably a consequence of the model geometry, characterised by a delta wing - the more so as it was small compared with the body dimensions. Anyhow, this confirms previous results, obtained in other wind tunnels (see, e.g., [15]).

In subsonic regime CL-α curves do not appear to be affected by blockage effects, as it can be seen by analysing, as an example, fig. 4-a (M=0.3). In transonic regime differences are, again, very small at low angles of attack (up to 10 degrees), while more pronounced differences appear for higher angles of attack; this behaviour was found

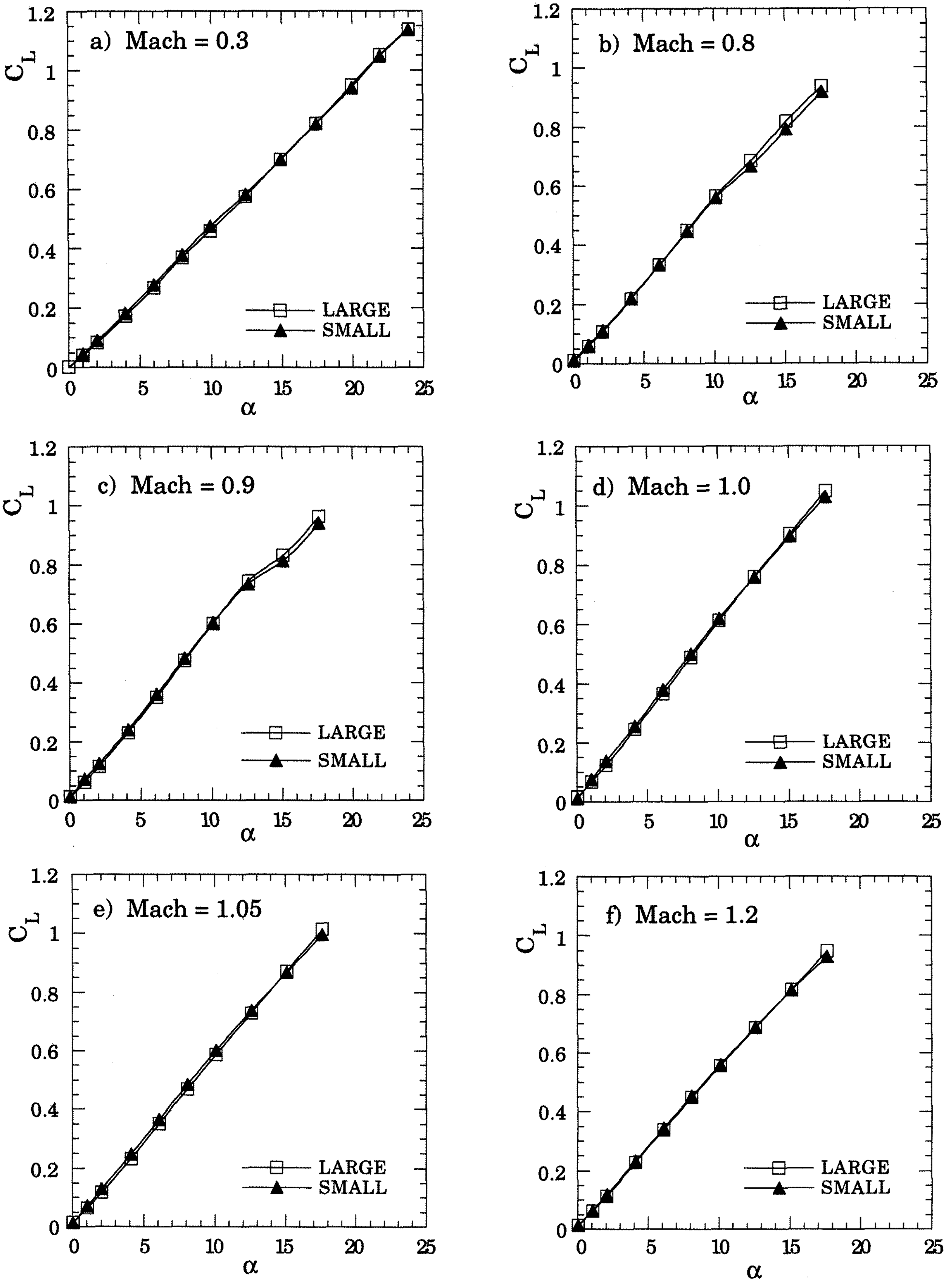

Fig. 4 - Lift versus angle of attack, for different Mach numbers

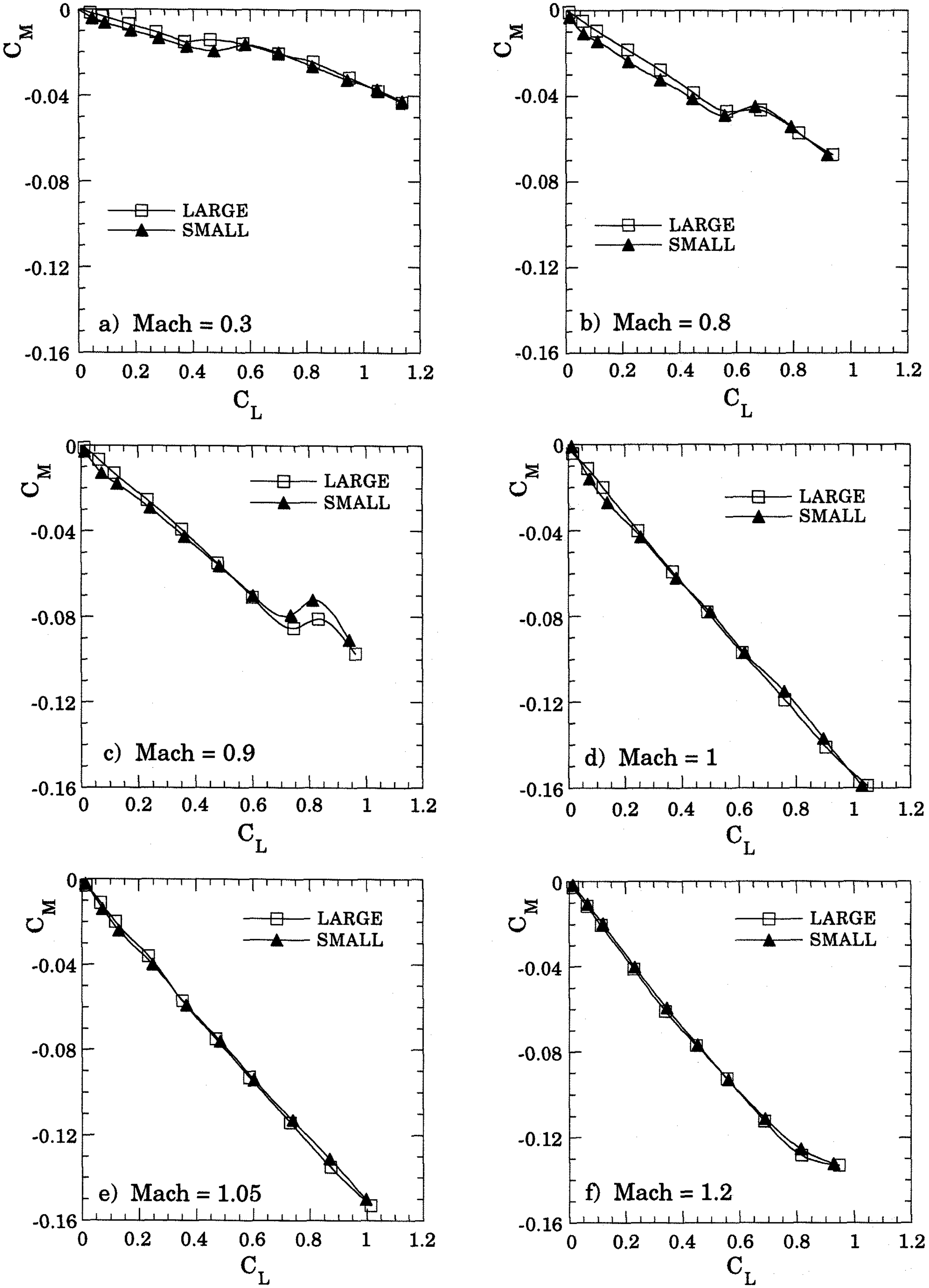

Fig. 5 - Pitching Moment versus Lift, for different Mach number

for M=0.8 to 0.9 (figs. 4-b and c), while for M=1 and 1.05 (figs. 4-d and e) the behaviour was different. In fact, small differences were observed at any considered angle of attack, which were, however, of the same order as measurement uncertainty, and therefore did not evidence any blockage effect, on lift characteristics when crossing to sonic free-stream conditions. Any difference disappeared, at the investigated angles of attack, at supersonic free stream, as shown in fig. 4f, (M=1.2). Thus, it appeared that at high angles of attack, in low transonic regime, significant blockage effects were present on lift characteristics, while less important effects were present from M=0.95 to M=1.1 - effects that tended to disappear as Mach number increased.

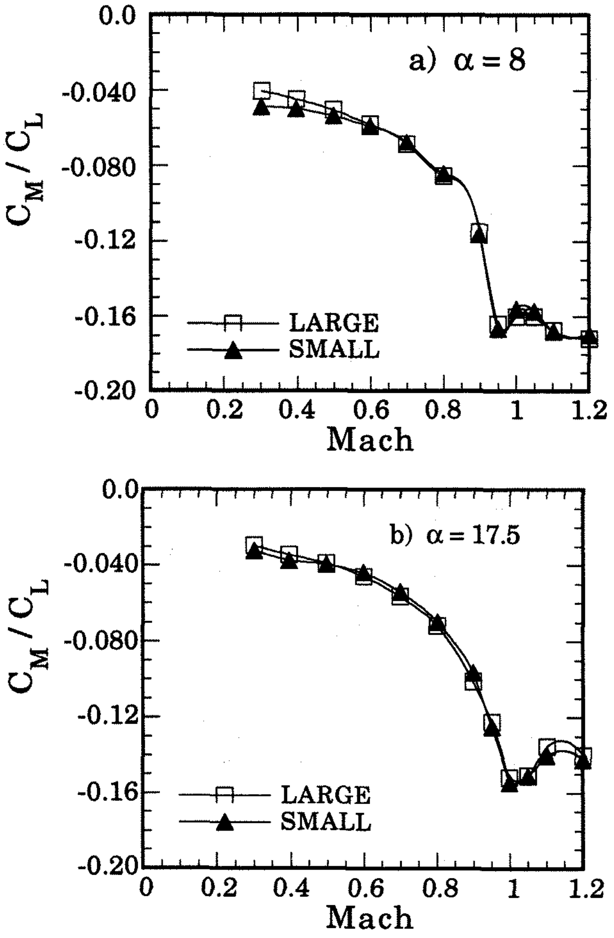

Fig. 6 - Pitching Moment to Lift ratios versus Mach number, for different angles of attack

However, it is very interesting to note that the effects on lift were strongly correlated with those on the pitching moment. Fig. 5 shows the moment coefficient C_M versus C_L, for the Mach numbers previously considered; only very localised differences can be observed, corresponding to the inflexion point in the curves, and, furthermore, they are particularly prominent at the lower Mach numbers. Since measurement uncertainty is higher in subsonic regime (tabs. 3 and 4), because forces are smaller, it is then possible that such differences derive from measurement uncertainty, which is known to be particularly important in moment evaluation. The correlation between lift and pitching moment is confirmed by analysing fig. 6, which shows, as an example, the variation of the C_M/C_L ratios with the Mach number, for angles of attack of 8 and 17.5 degrees: the curves are almost perfectly superimposable, except in the subsonic regime, where some differences are present. It is therefore very probable that blockage effects on moment evaluation were present, but they had the same origins as those related to the lift ones - which is why they disappear when longitudinal stability is studied as a function of lift characteristics. As to the low subsonic regime, no definite conclusions can be achieved, because the differences in the two model measurements are not large enough to be surely attributable to blockage effects.

Drag characteristics can be analysed as zero lift drag and lift dependent drag. The lift dependent drag (fig. 7) shows, for any Mach number, a very surprising coincidence for the two models, also characterised by an almost linear correlation between the C_L^2 and the C_D-C_{Dmin} values. For a more detailed analysis, in fig. 8 the interpolated linear coefficient K between C_L^2 and C_D-C_{Dmin} is reported, as a function of the Mach number; differences are almost negligible, and there are very high values of the correlation factor - in any case higher than 0.995. Even in this setting, blockage effects are likely to occur when changing the angle of attack, but, again, they have the same origins as those related to lift - which is why they disappear when drag (as is usually the case) is studied as a function of lift.

The zero lift drag is difficult to predict, because of the small values of the forces involved, with a consequently high error level (tab. 5); an accurate analysis of the zero lift drag characteristics would require a different campaign test, with a completely different choice of test procedures. Anyhow, in fig. 9 the C_{D0}, as a function of the Mach number, is shown; differences are present, but they may be due to a Reynolds effect (in this case, a more laminar flow on the small model, affecting results in the way previously shown): indeed, this parameter is markedly affected by viscosity.

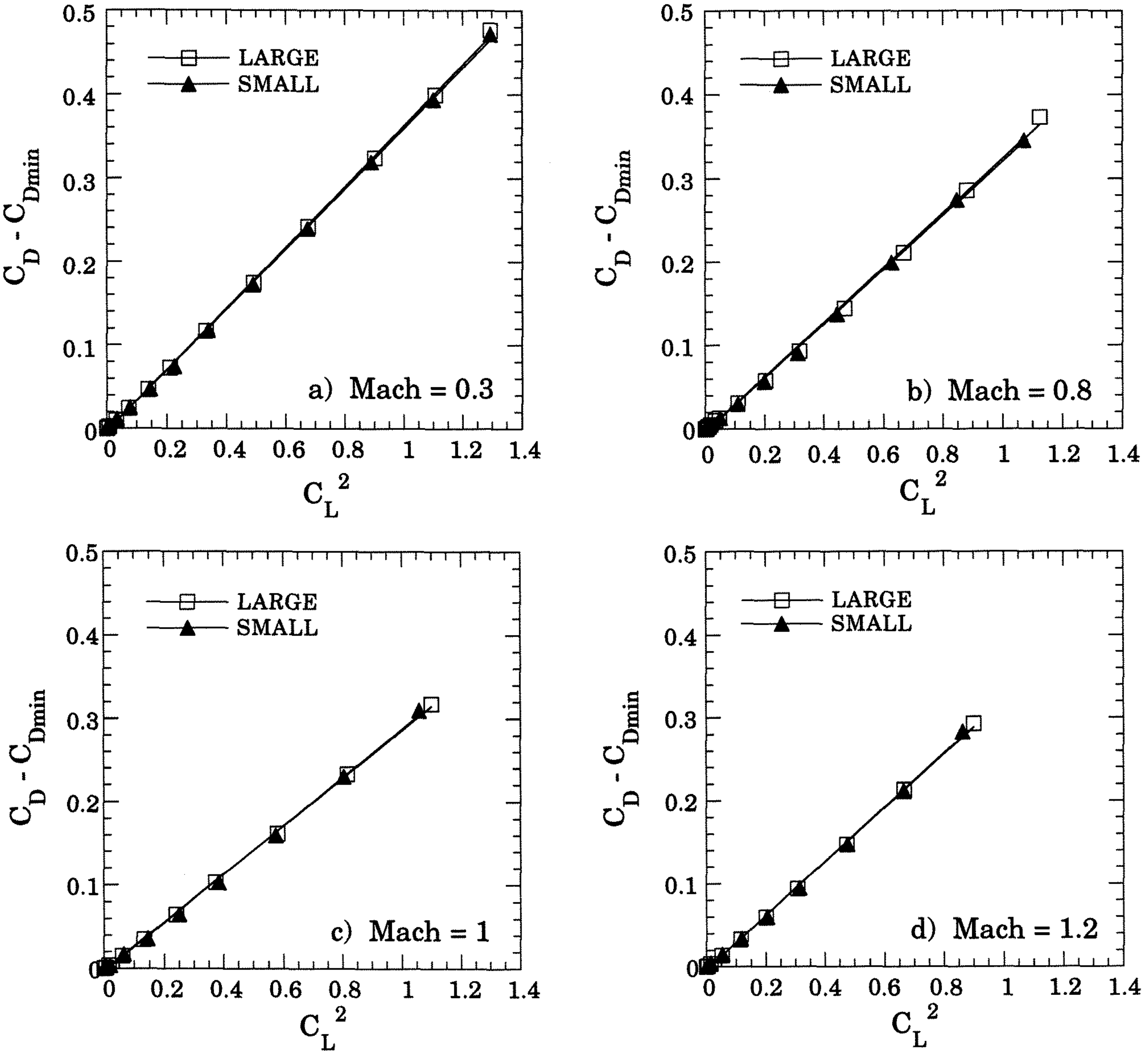

Fig. 7 - Drag-(Zero Lift Drag) versus squared Lift, for different Mach numbers

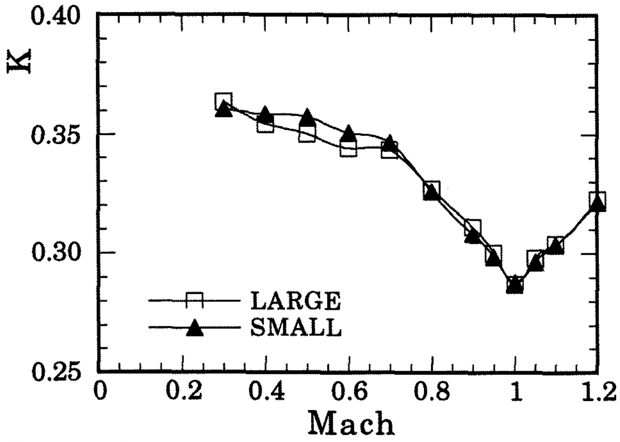

Fig. 8 - Linear K coefficient, relating incremental Drag to squared Lift, versus Mach number

In any case, differences are of the (high, in this case) uncertainty order, except for the higher Mach number where differences are more important - being significantly higher than uncertainty level. Thus, it is likely that, in supersonic flow conditions, a blockage effect affecting zero drag measurements was present, while no definite conclusions are possible with respect to the other flow conditions. However, it is of interest that the evaluation of the drag rise Mach number does not appear to be affected by model scale (fig. 9).

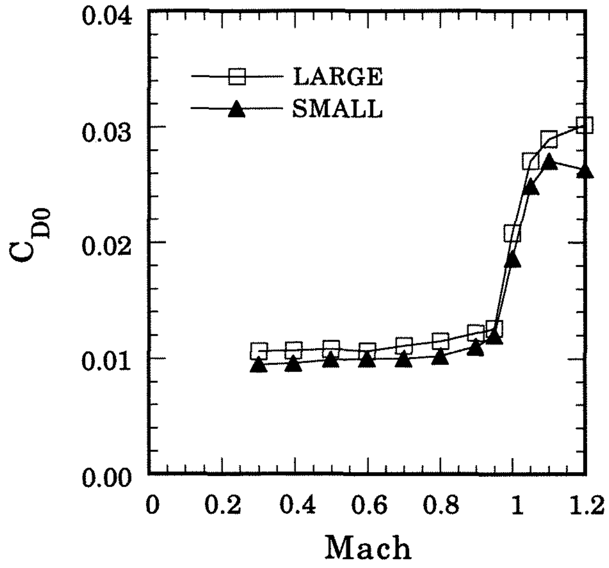

Fig. 9 - Zero Lift Drag versus Mach number

Conclusions

The use of different scale models, operating in a given wind tunnel under identical flow conditions, appears to be the most appropriate procedure to gain information on wall interference effects; in fact, this approach abolishes any differences related to different flow conditions, and the uncertainty in measurement comparisons is considerably reduced - being limited to the random component (which can be reduced, theoretically, to any desired values) of the measurement procedure as well as to the bias uncertainty related to balances.

The present research activity addressed wall interference effects on longitudinal aerodynamic characteristics, especially as related to pressure-dependent forces. An accurate analysis of the zero lift drag would actually require a specialised test campaign, with an appropriate choice of instruments and testing techniques.

The test section geometry is very close to that generally suggested as the design producing a wall interference-free environment for moderately sized models -such as the "large" model used here may be considered. The results presented in this paper would confirm that this solution is able to significantly reduce wall interference effects, particularly in the very critical conditions of Mach numbers close to one.

However, in some flow conditions, despite the moderate dimensions of the "large" model, wall interference effects are probably present. In particular, the pressure dependent forces appear to be affected by blockage effects at high angles of attack in the low transonic regime (M 0.7-0.95). However, since blockage effects on pressure actions were likely to be caused by the same factors, they tended to disappear when longitudinal stability and lift dependent drag were studied as a function of lift characteristics.

Another parameter that may be considered affected by blockage effects is the zero lift drag in the supersonic regime, while no definite conclusions can be reached in the subsonic regime, since the measurement procedure adopted is not sufficiently accurate for evaluating the zero lift drag. However, it should be observed that the drag rise Mach number evaluation appears to be fully free of blockage effects.

In summary, when a model with dimensions comparable with the "large" one is utilised in a test section like the one used here (which is typical for the latest transonic wind tunnels), it can probably be considered not affected by significant blockage effects - though but with respect to lift characteristics and not to the angles of attack. In any case, it appears that the above dimensions should be considered the largest acceptable for industrial applications, even though they are probably not sufficiently small if high accuracy is required.

References

[1] Vayssaire, J.C., "Survey of Methods for Correcting Wall Constraints in Transonic Wind Tunnels", in AGARD Report No. 601, "Problems in Wind Tunnel Testing Techniques", Apr. 1973.

[2] Bengelink, R.L., Zinserling, N.J., "Wall Interferences Measurements for Three-Dimensional Models in Transonic Wind Tunnels: Experimental Difficulties", in NASA CP 2319, 1984.

[3] Ashill, P.R., "Boundary-Flow Measurements Methods for Wall Interference Assessment and Correction - Classification and Review", 73rd AGARD Fluid Dynamics Panel Meeting and Symposium on Wall Interference, Support Interference and Flow Field Measurements, Brussels, Oct. 1993.

[4] Ferri, A., Baronti, P., "A Method for Transonic Wind-Tunnel Corrections", AIAA Journal, Vol.11, No.1, pags. 63-66, Jan. 1973.

[5] Monti, R., "Wall Corrections for Airplanes with Lift in Transonic Wind Tunnel Tests",

Report of the AGARD Ad Hoc Committee on Engine - Airplane Interference and Wall Corrections in Transonic Wind-Tunnel Tests, AGARD AR 36, 1971.

[6] Vaucheret, X., Vayssaire, J.C., "Corrections de Parois en Ecoulement Tridimensionnel Transsonique dans des Veines a Parois Ventilèes", 73rd AGARD Fluid Dynamics Panel Meeting and Symposium on Wall Interference, Support Interference and Flow Field Measurements, Brussels, Oct. 1993.

[7] "Specification for the AGARD Wind Tunnel Calibration Models", AGARD Memorandum AG-4/M3, Aug. 1955.

[8] "A Review of Measurements on AGARD Calibration Models", AGARDograph 64, Nov. 1961.

[9] Ongarato, J.R., "Wind-Tunnel Wall Interference Studies at High Subsonic Speeds", Journal of Aircraft, Vo.6, No.2, pags. 144-149, Mar.-Apr. 1969.

[10] Otto, H., "Systematical Investigations of the Influence of Wind-Tunnel Turbulence on the Results of Model Force-Measurements", in AGARD CP 174, "Wind Tunnel Design and Testing Tecniques", Oct. 1975.

[11] Hurlin, R.S., Davis, M.W., "Preliminary Calibration Results for the CSIR Medium Speed Wind Tunnel", DAST Report 90-320, Nov. 1990.

[12] Christison, R., "Dimensional Inspection Report", Projects Expedited (PTY) LTD Calibration Equipment, Book 1, 1988. (available at MSWT-CSIR).

[13] Davis, M.W., "Analysis of Pressure Measurement Error as Applied to the Static-Pipe Calibration of MSWT", presented to the 26th Subsonic Aerodynamic Testing Association, Torino, May. 1990.

[14] Coleman, H.W., Steele, W.G., "Experimentation and Uncertainty Analysis for Engineers", John Wiley & Sons, New York, 1989.

[15] Anderson, C.F., "An Investigation of the Aerodynamic Characteristics of the AGARD Model B for Mach numbers from 0.2 to 1.0", AEDC-TR-70-100, May 1970.